Applied Energy 285 (2021) 116392

Contents lists available at ScienceDirect

Applied Energy

journal homepage: www.elsevier.com/locate/apenergy

Seasonal storage and demand side management in district heating systems with demand uncertainty

Ruud Egging-Bratseth [a,*], Hanne Kauko [b], Brage Rugstad Knudsen [b], Sara Angell Bakke [a], Amina Ettayebi [a], Ina Renate Haufe [a]

[a] Department of Industrial Economics and Technology Management, Norwegian University of Science and Technology, Trondheim, Norway
[b] SINTEF Energy Research, Kolbjørn Hejes vei 1B, Trondheim 7491, Norway

ARTICLE INFO

Keywords:
District heating
Demand side management
Stochastic programming
Waste heat utilization
Thermal storage and flexibility

ABSTRACT

District heating is an under-researched part of the energy system, notwithstanding its enormous potential to contribute to Greenhouse Gas emission reductions. Low-temperature district heating is a key technology for energy-efficient urban heat supply as it supports an efficient utilization of low-grade waste-heat and renewable heat sources. The low operating temperature for such grids facilitates the integration of seasonal thermal energy storage, enabling a high degree of operational flexibility in the utilization of both uncontrollable and controllable heat sources. Yet, an inherent challenge of optimizing the operation of low-temperature district heating networks and its flexibility is the underlying uncertainty in heat demand. We develop a new stochastic model to minimize the total operational cost of district heating networks with local waste heat utilization, seasonal storage and uncertain demand. We consider in particular how demand side management and seasonal storage can improve the operational flexibility and thereby reduce costs. We analyze different set-ups of a local low-temperature district heating network under development in a new residential area in Trondheim, Norway. We find up to 37% reductions in carbon dioxide emissions, 29% generation reduction in peak hours, and 10% lower operational costs. These large values highlight the significance of flexibility options in low-temperature district heating networks for cost-effective, large-scale deployment.

1. Introduction

Space heating (SH) and hot water (HW) production for buildings account for approximately one fifth of global energy consumption [1]. Collective heating solutions have large potential to reduce the costs and emissions related to heating. In Europe, about half of the building heat demand could be met cost-efficiently by network heating systems (e.g.,Connolly et al. [2]). District Heating (DH) is advantageous because it enables economic utilization of energy sources that otherwise would go to waste. However, today's DH networks (DHNs) operate with high temperatures, causing high heat losses and limiting the utilization of low-temperature waste heat sources such as data centers, metro stations or other sources often present in urban areas [3]. Modern low-temperature DH, often referred to as 4th generation DH [4], will be designed with lower distribution temperatures to reduce heat losses and to enable efficient utilization of low-temperature waste heat and renewable heat sources.

An important component in 4th generation DH systems is thermal energy storage (TES). Incorporating TES in DH systems provides a wide range of energetic, economic and environmental benefits such as peak shaving, reduction in needed generation capacity, improved network flexibility management, and GHG emission reduction [5]. Short-term TES in the form of large HW accumulation tanks is the most common type of storage in DH systems [6]. This well-known and robust technology has low installation cost, high reliability, and short response times, and is generally easy to install and operate [5]. Seasonal TES based on large numbers of coupled boreholes is a less applied technology that is gaining popularity. Borehole TES has high losses during the first years of operation; however, these losses decrease significantly over time when the ground temperature stabilizes [7]. Seasonal borehole TES systems have been implemented in DH systems utilizing heat sources that have their largest generation in the summertime, such as solar thermal [8]. Similarly, due to low demand, DH systems with generation from municipal or industrial waste incineration often have large amounts of excess heat in summer (e.g., Nordell et al. [9]), which could be stored in a seasonal TES, and extracted during winter.

Integrating and utilizing several types of energy sources and TES in a DHN increases its complexity and it is challenging to cost-efficiently manage operation of the network. DH operators need tools to support

* Corresponding author.
E-mail address: ruud.egging@ntnu.no (R. Egging-Bratseth).

https://doi.org/10.1016/j.apenergy.2020.116392
Received 30 June 2020; Received in revised form 26 November 2020; Accepted 19 December 2020
Available online 7 January 2021

their tactical planning and operation. This paper presents an optimization method and benefits of optimally operating low-temperature DHNs. After a brief literature review, we describe our mathematical model developed for optimal scheduling and operation planning under uncertainty, and analyze how flexibility options enabled by seasonal storage and demand side management (DSM) affect operations and reduce costs and GHG emissions.

To the best of our knowledge, only few papers propose optimization models combining DSM and seasonal TES in DHNs. Similarly, few studies account for uncertainty in demand when modeling the operation of DHNs. We address this gap with our model that seeks to minimize the expected operational cost to meet uncertain demand considering the costs for different heat production technologies, DSM techniques, seasonal TES, and local waste heat.

2. Literature overview

Heat generation capacity and transportation network capacity in a DHN should be able to meet peak demand and constitute the major determinants of initial network investment cost. Peak generation often has high operational cost and carbon emissions. As such, both investment and operational costs, as well as emissions, benefit from peak load reduction. Therefore, the majority of DHN research focuses on ways to reduce the peak load.

Security of supply and operational flexibility in DH systems can in general be achieved by three means: (i) a diverse, appropriately dimensioned portfolio of heat generation units (boilers), (ii) TES, and (iii) DSM. The heat generation portfolio must have sufficient redundant capacity to provide backup generation when needed, while diversifying the boilers concerning fuel needs (e.g., biomass, natural gas and electricity), allows hedging against demand and price variations. TES can be used to absorb surplus (waste) heat and to maximize the generation from lowest cost boilers, to reduce generation from high cost boilers. DSM can reduce the generation needs in peak periods by reducing demand or shifting load to adjacent periods, often at a penalty.

Vandermeulen et al. [10] analyzed how different TES types can help unlocking the flexibility in DHNs to facilitate renewable energy sources (RES) integration in the broader energy system. Leśko et al. [11] explored characteristics, such as size and location, for TES in a DHN to maximize flexibility at the lowest cost. They concluded that conventional HW tanks are the lowest cost solution. Verrilli et al. [12] considered the problem of scheduling boilers, TES, and flexible loads in DHNs using model predictive control. By optimizing operations over a receding horizon, they adjust for changing weather predictions and short-term uncertainty in demand. Knudsen and Petersen [13] considered price-based demand response of residential heat pumps in ultra-low temperature DHN, using model predictive control. Vivian et al. [14] studied the use of storage capacity and adjustment of the flow rate in a DHN in Verona, Italy, as a flexibility measure for balancing generation needs. Zheng et al. [15] considered the thermal inertia of DHNs as a flexibility source for scheduling combined heat and power (CHP) plants, thereby improving the ability of integrating RES. As an alternative to model-based optimization methods, Claessens et al. [16] considered a reinforcement-learning type approach for operating flexible thermostatically controlled loads in DHNs.

DSM for DHNs seeks to reduce the heat production and supply costs through load management (e.g., [17,18]). Guelpa et al. [19] considered peak reduction through DSM for the DH system in Turin, Italy. By minimizing the maximum daily load and anticipating loads of the buildings connected to the network, they reduced peak loads by about 5%. The potential reduction in energy costs by using DSM in an urban, conventional DHN in Denmark was investigated by Cai et al. [20]. The authors allowed flexibility in space and HW supply, with no-cost upward temperature adjustments in HW tanks above a lower bound, while deviations outside an SH comfort zone were penalized. The results indicated a potential of 11% reduction in energy costs. Sweetnam et al. [21] considered residential demand response on DHNs to improve the load factor (the ratio of daily mean and maximum heat demand). A higher load factor implies a flatter load profile, and thus lower network investment costs. In a field trial in the United Kingdom, the authors reported an increase in load factor from 29% to 44% and significant network cost savings, however at the expense of a 3% demand increase. Recent publications have reported experiments with demand shifting, both in homes [22] and in commercial and office buildings [23].

Besides approaches based on optimization over a receding horizon, e.g. Verrilli et al. [12] and Knudsen and Petersen [13], few references address explicitly the inherent uncertainty in DH operations caused by weather conditions or building occupants behavior. Hohmann et al. [24] presented a two-stage stochastic optimization problem for operation of DHNs with uncertain demand. The authors presented a control-oriented approach to minimize expected operational cost incurred by hydraulic and thermal losses with respect to a uncertainty in heat demand. No DSM or particular flexibility measures were considered, and all uncertainty resolved in the second stage. Other recent publications address uncertainty related to CHP operation, e.g. uncertainty in biomass supply [25] or wind generation [26], affecting the dispatched heat production and delivery.

Table 1 summarizes components and methodology of related literature to the problem and approach we consider in this paper. The reviewed literature indicates the lack of approaches that explicitly consider uncertainty in scheduling and operational optimization and flexibility measures in DHNs. This is particularly the case for low-temperature DHNs with waste-heat sources and seasonal TES. In this paper we aim to address this gap in the literature, by developing a multi-stage optimization approach, considering load uncertainty, TES and DSM.

Table 1
Selected articles addressing DHN optimization.

Authors	Det/Sto	Components	Objective
[12]	Det	DH/TES	Min energy cost
[20]	Det	DH/DSM	Min energy cost
[27]	Det	DH/TES	Min total cost & CO_2 emission
[19]	Det	DH/DSM	Min thermal peak
[24]	Sto	DH	Min operational cost
[11]	Det	DH/TES	Min operational cost
[28]	Det	DH/EL/PV/CHP	Min total cost
[29]	Det	DH	Min operational cost
Our contribution	**Sto**	DH/DSM/TES	**Min operational cost**

Table 2
Sets, indices and their representation in the optimization model.

Indices and Sets:	
$e \in E$	Set of all heat production technologies.
$E^C \subset E$	Set of controllable heat technologies.
$E^U \subset E$	Set of uncontrollable heat technologies.
$g \in G = \{SH, DHW\}$	Set of demand types.
$i, j \in N$	Set of all nodes.
$N^P \subset N$	Set of heat central nodes.
$N^B \subset N$	Set of branching nodes.
$N^C \subset N$	Set of consumer nodes.
$t \in T^S = \{1, 2, \ldots, t^S_{last}\}$	Set of strategic time periods.
$h, h' \in T^O = \{1, 2, \ldots, t^O_{last}\}$	Set of operational time periods.
$p \in P$	Set of all user profiles.
$\omega \in \Omega$	Set of all operational scenarios

3. Model formulation

To support the tactical-operational planning of a broad range of DHNs, the model formulated here can account for the relevant characteristics of DHNs, and handle different network layouts, production technology mixes, loads with different profiles, DSM, and TES. The objective is to minimize (expected) variable operating costs including

Table 3
Parameters used in the optimization model.

Parameters:	
$C_{ghh'p}$	Cost for unmet demand of type g in the operational period from h to h' for user profile p.
C^A	Unit cost for adding heat to the TES.
C^E_e	CO_2 emission cost for technology e.
C^F_{eth}	Unit fuel costs of technology e in strategic period t at operational period h.
C^T_{ij}	Pipeline transportation costs from node i to node j.
COP^C	Coefficient of performance (COP) for the centralized heat pump.
COP^D	COP for the decentralized heat pumps.
$D_{githp\omega}$	Target demand for type g at node i in strat. period t, oper. period h for profile p in scenario ω.
$L_{gihh'p}$	Minimum percentage of demand that must be satisfied.
$U_{gihh'p}$	Maximum percentage of demand that can be satisfied.
F^{MAX}_{ij}	Capacity for the pipeline from node i to j.
O_e	CO_2 emission factor for technology e.
Q^{-MAX}_{it}	Capacity limit for adding heat to the TES at node i in strategic period t.
Q^{+MAX}_{it}	Capacity limit for withdrawing heat from the TES at node i in strategic period t.
S^{MAX}_i	Total inventory[a] capacity limit for TES at node i.
R_{ip}	Percentage of demand at node i from user profile p.
X_{eith}	Uncontrollable heat supply by technology e at node i in strategic period t in operational period h.
X^{MAX}_{eith}	Production capacity for technology e at node i in strategic period t in operational period h.
η_{ij}	Efficiency ratio (1-loss rate) for heat flow from node i to node j.
η^A	Efficiency ratio for adding heat to the TES.
η^S_t	Efficiency ratio for the stored heat in the TES from strategic period t to $t+1$.

[a]Inventory is the TES charge, the total amount of heat stored in seasonal storage.

emissions costs and penalties for demand shifting and curtailment. Decisions for every period in the planning horizon are: heat production from each controllable technology, heat additions to and withdrawals from TES respectively, and actual, deficit and surplus supply to each consumer. We consider operational decisions only, not investments. Different types of consumers have different load profiles for SH and HW. These profiles can be uncertain, which is represented as different demand values that may occur with known probabilities. We impose a structure of strategic periods with embedded operational periods. To allow a linear model, we impose fixed operating temperatures for different parts of the grid, heat losses independent from ambient temperatures, and disregard any start-up costs for dispatching generation technologies or connected to seasonal TES.

Table 2 summarizes sets and corresponding indices, Table 3 parameters and Table 4 variables used in the optimization model.

The objective is to minimize the total expected operational costs in Eq. (1). The first term is the production costs for controllable technologies, the second term is the transportation cost, while the third term is the total deficit cost. The fourth term is the cost associated with TES operations, while the two last terms are the electricity cost for heat pumps connected to DHW supply and uncontrollable technologies, respectively. All scenario-dependent terms are multiplied by the probability of each scenario, π_ω. Furthermore, the scenario-dependent costs are summed over all scenarios $\omega \in \Omega$. The last term is not scenario dependent; it represents the cost to lift the temperature of the uncontrollable waste heat to the network operation temperature, and is in fact a fixed cost.

$$\begin{aligned}\min \sum_{\omega\in\Omega}\pi_\omega \sum_{t\in T^S}\sum_{\substack{h,h'\in T^O\\ \wedge h'\geq h}} \Bigg(& \sum_{e\in E}\sum_{i\in N}(C^F_{eth}+C^E_e O_e)x_{ith\omega} \\ & + \sum_{i\in N}\sum_{j\in N} C^T_{ij} f_{ijth\omega} + \sum_{g\in G}\sum_{i\in N^C}\sum_{p\in P} C_{ghh'p} z_{githh'p\omega} \\ & + \sum_{i\in N} C^A q^-_{ith\omega} + \sum_{i\in N}\sum_{p\in P} C^P_{(EL),th}\frac{y_{(DHW),ithp\omega}}{COP^D}\Bigg) \\ & + \sum_{i\in N}\sum_{t\in T^S}\sum_{h\in T^O} C^P_{(EL),th}\frac{X_{eith}}{COP^C}\end{aligned} \tag{1}$$

CO_2 emissions in (1) are in kg, emission cost in NOK/kg, emission factor in kg CO_2/kWh, while all other volumes and costs in kWh and NOK/kWh, respectively. All variables are non-negative.

Demand constraints

Constraint (2) defines deficit loads as the difference in heat demand and delivered heat over the operational periods. We impose this as an inequality constraint as surplus deliveries of heat cause the right-hand side to become negative.

$$z_{githh'p\omega} \geq \sum_{\tau=h}^{h'}(R_{ip}D_{git\tau p\omega} - y_{git\tau p\omega}),$$
$$\forall g\in G, i\in N^C, t\in T^S, (h,h')\in T^O \wedge h'\geq h, p\in P, \omega\in\Omega \tag{2}$$

Constraint (3) and (4) ensure that the delivered heat covers the minimum requirements in the consecutive operational periods, but not more than the maximum deliverable amount.

$$\sum_{\tau=h}^{h'} y_{git\tau p\omega} \geq L_{gihh'p}R_{ip}D_{githp\omega},$$
$$\forall g\in G, i\in N^C, t\in T^S, (h,h')\in T^O \wedge h'\geq h, p\in P, \omega\in\Omega \tag{3}$$

$$\sum_{\tau=h}^{h'} y_{git\tau p\omega} \leq U_{gihh'p}R_{ip}D_{githp\omega},$$
$$\forall g\in G, i\in N^C, t\in T^S, (h,h')\in T^O \wedge h'\geq h, p\in P, \omega\in\Omega \tag{4}$$

Production capacity

Production from a controllable technology cannot exceed its capacity.

$$x_{eith\omega} \leq X^{MAX}_{eith}, \qquad \forall e\in E^C, i\in N^P, t\in T^S, h\in T^O, \omega\in\Omega \tag{5}$$

Nodal heat balance

The heat balance for each node i is given in Constraint (6), with the sum of heat sources and inflows on the left side and the sum of outflows and sinks on the right. The sources are produced heat from controllable and uncontrollable technologies, heat inflow from connected nodes (corrected for heat losses) and heat withdrawn from TES. The sinks are delivered heat, heat outflow to connected nodes and heat added to TES.

$$\begin{aligned}&\sum_{e\in E^C} x_{eith\omega} + \sum_{e\in E^U} X_{eith} + \sum_{j\in N}\eta_{ji}f_{jith\omega} + q^+_{ith\omega} \\ &= \sum_{g\in G}\sum_{p\in P} y_{githp\omega} + \sum_{j\in N} f_{ijth\omega} + q^-_{ith\omega}, \\ &\forall i\in N, t\in T^S, h\in T^O, \omega\in\Omega\end{aligned} \tag{6}$$

Pipeline capacity limit

Constraint (7) ensures that transported heat respects the pipeline capacities.

$$f_{ijth\omega} \leq F^{MAX}_{ij}, \qquad \forall (i,j)\in N, t\in T^S, h\in T^O, \omega\in\Omega \tag{7}$$

Table 4
Optimization variables.

Variables:	
$f_{ijth\omega}$	Heat amount transported from i to j in strategic period t in operational period t in scenario ω.
$q^{-}_{ith\omega}$	Heat amount added to TES at node i in strategic period t in operational period h in scenario ω.
$q^{+}_{ith\omega}$	Heat amount withdrawn from TES at node i in strategic period t in operational period h in scenario ω.
$s_{ith\omega}$	Heat inventory in TES at node i in strategic period t at the end of operational period h in scenario ω.
$x_{eith\omega}$	Heat amount produced by technology e at node i in strat period t in oper. period h in scenario ω.
$y_{githp\omega}$	Delivered heat to demand type g in node i in strat period t, oper period h for profile p, scenario ω.
$z_{githh'p\omega}$	Deficit for demand type g in node i in strat period t, oper periods h to h' for profile p in scenario ω.

Table 5
Heat generation capacities (kWh/h).

Month	Waste incineration	Bio boiler	Electric boiler	LPG	NG
January	0	1 733	688	10 000	0
February	0	1 684	516	10 000	0
March	0	1 900	507	10 000	0
April	0	1 636	413	10 000	413
May	1 568	0	10 000	0	10 000
June	1 468	0	0	0	0
July	1 317	0	0	0	0
August	1 162	0	0	0	0
September	1 043	0	10 000	0	10 000
October	0	1 179	522	10 000	522
November	0	1 397	565	10 000	565
December	0	1 521	552	10 000	0
Production cost	0.02	0.32	0.37–0.55	0.75	0.34

Storage constraints

The initial storage level in an operational period depends on the initial storage level and additions and withdrawals in the previous operational period, with corrections for losses where appropriate. In most operational periods, the previous operational period is within the same strategic period, and in these cases, Constraint (8a) applies. Constraint (8b) applies for the first operational period $h = 1$ in the first strategic period $t = 1$ in the planning horizon. Constraint (8c) applies for the first operational period in the other strategic periods. Like constraint (8a), they determine the TES inventory at the start of the operational period, but accounting for a heat loss between strategic periods.

$$s_{ith\omega} = s_{it(h-1)\omega} + \eta^{A} q^{-}_{ith\omega} - q^{+}_{ith\omega} \qquad \forall i \in N, t \in T^{S} \setminus \{1\},\ h \in T^{O}, \omega \in \Omega \tag{8a}$$

$$s_{i,1,1,\omega} = \eta^{A} q^{-}_{i,1,1,\omega} - q^{+}_{i,1,1,\omega} \qquad \forall i \in N, \omega \in \Omega \tag{8b}$$

$$s_{it,1,\omega} = \eta^{S}_{t} s_{i(t-1)t^{O}_{last}\omega} + \eta^{A} q^{-}_{it,1,\omega} - q^{+}_{it,1,\omega} \qquad \forall i \in N, t \in T^{S}, \omega \in \Omega \tag{8c}$$

As the temperature from waste-heat streams used in low-temperature DH networks are low, adding waste heat to a TES may have the adverse effect of decreasing the storage temperature. To prevent this, Constraint(9) allows restricting the technologies that can store heat in TES.

$$\sum_{e \in E^{U}} X_{eith\omega} \geq q^{+}_{ith}, \qquad \forall i \in N, t \in T^{S}, h \in T^{O}, \omega \in \Omega \tag{9}$$

Capacity constraint (10) limits the total amount of heat that can be stored in a TES.

$$s_{ith\omega} \leq S^{MAX}_{i}, \qquad \forall i \in N, t \in T^{S} \setminus \{t^{S}_{last}\}, h \in T^{O} \setminus \{t^{O}_{last}\}, \omega \in \Omega \tag{10}$$

Capacity constraints (11) and (12) ensure that heat additions and withdrawals of heat to a TES respect capacity limits.

$$\eta^{A} q^{-}_{ith\omega} \leq Q^{-MAX}_{it}, \qquad \forall i \in N, t \in T^{S}, h \in T^{O}, \omega \in \Omega \tag{11}$$

$$q^{+}_{ith\omega} \leq Q^{+MAX}_{it}, \qquad \forall i \in N, t \in T^{S}, h \in T^{O}, \omega \in \Omega \tag{12}$$

The continuous, stochastic optimization model represented by Eq. (1)–(12) yields a, potentially very large, multi-stage, linear stochastic programming problem.

4. Case study

Owing to the operational temperature requirements to supply old, poorly insulated, buildings, the transition to low-temperature DHNs will start in areas with new or renovated buildings with more moderate space heating demand [30]. This study focuses on a new residential area, Leangen, to be developed in the eastern part of Trondheim, Norway. In Leangen, low-temperature waste heat is available from a nearby indoor ice rink. The available waste heat will, however, not be sufficient to cover the entire local load. Therefore, heat from the primary, high-temperature DHN in Trondheim will be needed in addition. The base heat supply for the primary DHN is a large waste incineration plant south of Trondheim, with large amounts of excess heat in the summertime. Although a seasonal TES is not foreseen in current plans for Leangen, it would be a flexibility option to store excess heat in summer, and supply this in winter months. The other flexibility option we investigate in this paper is DSM, where we allow both demand shifting and curtailment.

In the analysis we consider uncertainty in SH loads (but not in HW loads). The local DHN is represented by one heat central node, five branching nodes, and nineteen consumer nodes, as shown in Fig. 1. The network includes a local waste heat source and may include a seasonal TES, both of which are coupled to the heat central node. There are five building types (with aggregated average demand shares in parentheses): apartments (82.8%), nursing home (9.1%), kindergarten (1.5%), offices (4.3%) and stores (2.3%). The consumer types have different demand patterns and are hence considered as different load profiles. The local ice rink can cover approximately 22% of the expected heat demand at Leangen, according to data for 2019. For additional heat supply, the heat central node has a connection to the primary DHN of Trondheim. This primary DHN has five heat sources: waste incineration, and four controllable boilers using electricity, biomass, natural gas (NG), or liquefied petroleum gas (LPG).

We consider a planning horizon of one year. As strategic periods, we consider months. This means that at the end of each month uncertain information can become known. Each month is included as a representative day. As operational periods within each month, we include 24 h. The uncertainty in operational periods concerns the SH demand, which is further explained in the next section.

The monthly production capacities of the controllable heat sources available to supply heat to Leangen, are scaled based on the actual

Fig. 1. Architectural illustration of the Leangen area, with the modeled DHN overlaid, including: heat central (node 1 in blue), five branching nodes (nodes 2–6 in orange), and 19 consumer nodes (nodes 7–25 in green).

production mix from the Trondheim DHN in 2019, see Table 5. In the period May–September, there is surplus heat from waste incineration in Trondheim which is available for the Leangen DHN. This surplus heat can cover all demand in the summer months (i.e., June, July, and August) and provide base load in May and September. In other months, heat from waste incineration is fully utilized within the Trondheim DHN itself.

To illustrate the operation of DSM and TES, the capacity of peak load technologies is defined as the difference between average and minimum demand in the Leangen DHN. The electric boiler can be used to meet peak loads from October to April. Both electric boiler and NG may be used in May and September to cover peak load in scenarios with very high demand. LPG capacities ensure that the model is feasible for all demand scenarios. The bottom line of the table indicates the heat production costs [NOK/kWh produced].[1]

More details for production costs [NOK/kWh produced] are shown in Table 6. For each production technology, we list fuel costs and carbon emission cost. The latter are based on the carbon emission factors, multiplied by a CO_2 fee of 0.5 NOK/kg. The waste heat from the local ice rink does not incur fuel or emission cost, but its temperature must be lifted several degrees to bring it to operating temperature for the local DHN. This is done with dedicated heat pumps, that run on electricity. Electricity prices vary hourly (see fuel cost in the row for Electric boiler in Table 5).

The fuel costs are inferred from production technologies with capacities close to the real capacities of the main DHN in Trondheim [31]. Fuel costs for waste incineration, bio boiler, LPG, and NG are considered constant for the entire planning horizon. Hourly electricity costs are based on monthly and hourly averaged spot prices for power in Trondheim for the years 2013–2019 [33]. This results in hourly production cost for the electric boiler in the range from 0.3736 to 0.5529 NOK/kWh.

The low-temperature DHN at Leangen will be compact with a total length of 1300 meters only. Thus, heat losses in the pipelines will be small and the pumping work for heat transportation will be low. For these reasons, we ignore transportation losses and costs. Additionally, capacity limits on pipelines are ignored. The seasonal TES will be placed in the vicinity the heat central. Due to a high number of boreholes, and thus high thermal inertia in a seasonal TES, there are only two operational modes during a year. During the summer (June–August) it is only possible to add heat to the TES, and in the months from September to May heat can only be withdrawn from the TES. The operational costs and losses for adding heat to the TES are ignored. The year-round efficiency of seasonal TES is approximately 60% [34]. We implement a monthly loss rate on the heat inventory in the TES of 5.5%.

A central heat pump is responsible for lifting the temperature of local waste heat to the grid operating temperature. In addition, every consumer node has a (decentral) heat pump to lift the temperature for supplying HW. The coefficient of performance (COP) for the central heat pump, which lifts the temperature from 35 °C to 40 °C, is set to 10, while the COP for the decentralized heat pumps lifting the temperature from 40 °C to 55 °C is set to 5. The power cost for the heat pumps is the same as the production cost for the electric boiler.

We assume that HW storage tanks at consumer nodes can act as buffers, allowing for an hourly heat supply deficit and surplus of up to 20% for each user profile; total HW demand during a day must be met though. For SH, the hourly deficit and surplus vary dependent on the user profiles. If curtailment is allowed, this is at most 2% for each day.

Demand scenarios

The HW demand profile over a day is rather independent from outdoor temperatures. Fig. 2 shows the aggregate profile for all consumers combined.

From May to August, SH demand is low due to high outdoor temperatures, and can be met by cheap heat from waste incineration. Therefore, uncertainty in this period is not considered. To reflect uncertainty, we generate three different temperature scenarios (low, medium, and high) for each of the eight months in the period September–April. Starting point for the generation of temperature scenarios are the hourly temperatures for a year in Trondheim collected from the building simulation software SIMIEN [35]. Based on a K-means clustering algorithm, we divide each month with uncertain SH demand in three consecutive periods with the lowest, medium, and highest average temperature, c.f., Table 7.

For each period, we use the average hourly temperature over all days in the period to define three temperature scenarios; low, medium, and high, see Table 10 in Appendix.

[1] 1 NOK is about 0.12 USD.

Table 6
Production costs for different production technologies. [31,32].

Production technology	Fuel cost [NOK/kWh]	Carbon emission factor [kg/kWh]	Emission cost [NOK/kWh]	Production cost [NOK/kWh]
Waste incineration	0.0153	0.0112	0.0056	0.0209
Bio boiler	0.3140	0.0198	0.0099	0.3239
Electric boiler	0.3186–0.4979	0.1100	0.0550	0.3736–0.5529
LPG	0.6140	0.2740	0.1370	0.7510
NG	0.2200	0.2430	0.1215	0.3415

Table 7
Allocation of days to low, medium and high average temperature periods. Lowest average temperature periods are marked blue, highest average temperature orange, and medium average temperature green.

Day	Sep	Oct	Nov	Dec	Jan	Feb	Mar	Apr
1	13.8	3.0	−8.0	0.1	4.9	3.8	−0.1	−1.5
2	14.3	2.4	−5.8	−4.4	2.4	3.1	−1.3	−0.7
3	14.8	3.5	−3.8	3.6	2.6	0.6	−3.7	−2.4
4	16.8	4.9	−2.8	3.4	1.8	−7.4	−5.1	−0.2
5	15.8	6.0	−2.0	−0.6	0.3	−1.1	−4.4	5.8
6	13.2	6.2	−1.6	−1.9	−1.4	−2.5	−2.5	5.1
7	9.7	7.7	−0.4	−1.4	−0.3	−0.5	−2.8	8.3
8	11.4	5.7	3.6	0.5	−2.0	−3.7	−7.0	7.4
9	8.3	8.0	6.0	−2.5	−5.0	−8.7	−8.1	6.3
10	7.5	11.8	7.0	−0.3	−4.4	−5.1	−5.8	9.3
11	5.2	13.0	8.6	−6.2	−3.2	−4.1	−2.1	10.3
12	6.4	10.5	4.0	1.2	−16.2	−6.2	−3.3	7.0
13	7.0	9.9	1.6	−3.1	−10.9	−0.2	−1.7	3.7
14	12.3	9.4	2.1	2.4	−10.0	−13.1	−0.8	4.0
15	11.0	8.7	−0.7	3.0	−15.5	−11.3	0.7	2.8
16	10.5	5.3	1.2	6.3	−4.0	−3.0	1.2	2.3
17	4.5	7.0	2.6	2.2	−1.2	0.2	5.6	4.4
18	10.1	6.6	0.5	5.3	1.7	−4.5	2.8	0.8
19	8.6	4.2	7.7	4.7	4.1	−1.5	1.9	0.3
20	8.0	8.3	6.5	4.2	1.2	2.0	−0.4	1.5
21	9.9	7.4	4.4	−6.7	2.9	4.6	0.3	1.8
22	7.8	4.5	5.0	1.6	3.9	5.6	3.0	3.4
23	10.1	2.7	5.5	−5.5	0.8	1.2	1.6	4.0
24	12.7	3.8	−1.1	−11.0	−5.6	1.5	2.5	3.1
25	11.9	1.6	3.0	−14.6	−2.6	0.9	2.1	6.6
26	9.4	−0.9	0.9	−12.8	4.0	−2.0	1.0	5.5
27	9.1	0.4	0.0	−9.6	3.5	2.2	4.3	7.8
28	5.8	−1.8	−2.4	−8.3	0.7	2.7	4.0	4.7
29	9.6	1.0	−6.8	−3.8	1.9		3.4	2.1
30	8.7	2.0	−4.8	0.9	3.2		3.7	1.1
31		−0.2		−5.0	5.1		4.9	

The probability for each scenario (see Table 10 in the Appendix) equals the number of days in its underlying cluster divided by the total number of days in the specific month. This procedure implies that the represented uncertainty is asymmetric, with different probabilities for the low and high demand scenarios, and that the medium scenario values do not equal the averages.

Considering eight months with each three different outcomes, the scenario tree represented in the case study contains $3^8 = 6,561$ different scenarios in total.

5. Results

This section considers a Base Case without a TES or DSM, and case variants featuring flexibility options from DSM and a seasonal TES. In the Base Case, all demand must be met by production in the same hour. The flexibility options allow shifts in production on different time scales (within the day and between seasons) to avoid producing by the most expensive generation technologies and make more effective use of the cheaper ones.

We include a seasonal TES without capacity restrictions and investigate DSM by allowing different combinations of deficit and curtailment costs for SH demand. For HW demand we allow hourly deviations of 20% to reflect the presence of HW tanks in the buildings. We consider hourly deficit costs of 0.01 NOK/kWh (almost free) and 0.15 NOK/kWh. Surplus deliveries are not penalized. Curtailment costs are either 0.10 NOK/kWh or 0.20 NOK/kWh for not delivered heat. Since every curtailed kWh in a day is also a deficit in some hour of that day, actual curtailment costs are the sum of the (direct) curtailment costs and the hourly deficit costs. We implement cases wherein no curtailment is allowed by setting curtailment cost to 10 NOK/kWh. The cases with a seasonal TES allow higher production in summer months from biomass-fueled technology Bio boiler. Cases are denoted by BC for Base Case, and by Deficit Cost_Curtailment Cost for the other five.

To solve the data instances we use FICO® Xpress Optimization Suite version 8.8.1 on an Intel® E5-2643v3 processor at 3.4 GHz and 512 GB RAM. The computation time for each case is about 8 to 9 h.

Table 8 shows the aggregate results for the analyses. All case variants have about 10% lower expected costs, 29% lower peak generation (maximum generation in the coldest winter hour) and 36%–38% lower CO_2 emissions than the Base Case, with not much variation between them.

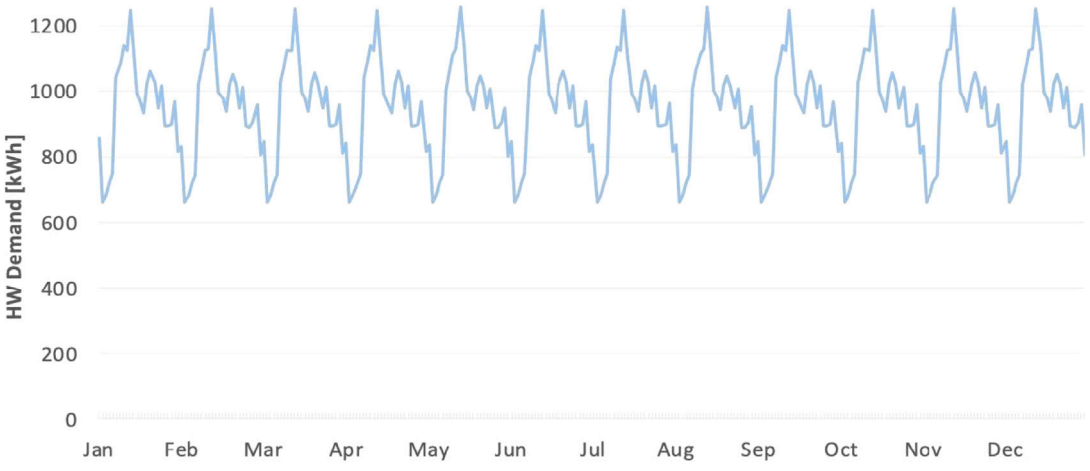

Fig. 2. Aggregate hourly HW demand profile for all representative days in a year.

Table 8
Summarized results. All values are expected values. Measurement units vary to accommodate inspection.

	Measurement unit	Base Case	Bio _0.01_10	Bio _0.15_10	Bio _0.01_0.2	Bio _0.15_0.2
Inputs						
Deficit costs	NOK/kWh		0.01	0.15	0.01	0.15
Curtailment costs	NOK/kWh		10	10	0.2	0.2
Outputs						
Total generation	MWh	646.3	667.3	667.5	658.4	660.8
Maximum inventory	MWh		80.7	81.9	73.9	75.2
CO_2 emissions	ton	27.4	17.6	17.5	17.1	17.3
Fuel costs	kNOK	143.4	126.2	126.3	123.3	124.0
Deficit costs	NOK		19.3	49.2	87.5	805.0
Curtailment costs	NOK		*N.A.*	*N.A.*	1430.9	1021.3
Heat Pump Central	kNOK	6.8	6.8	6.8	6.8	6.8
Heat Pump DHW	kNOK	26.4	26.2	26.2	26.2	26.2
Total shifted	kWh		3860	656	17500	10733
Total curtailed	kWh				7155	5107
Peak generation	kWh	3016	2141	2139	2141	2141
Total cost	kNOK	176.6	159.2	159.3	157.8	158.8
Total cost rel to BC	%		−9.8%	−9.8%	−10.7%	−10.1%
Total generation rel to BC	%		3.2%	3.3%	1.9%	2.2%
Peak generation rel to BC	%		−29.0%	−29.1%	−29.0%	−29.0%
CO_2 emissions rel to BC	%		−35.9%	−36.2%	−37.5%	−36.8%
Max inventory rel to prod	%		15.4%	15.6%	14.3%	14.5%
Shifted rel to production	%		0.6%	0.1%	2.7%	1.6%
Curtailed rel to production	%				1.1%	0.8%
Fuel cost rel to total cost	%	81%	79%	79%	78%	78%

Reported values are model results. To scale to full-year results these values should be multiplied by 30.5.

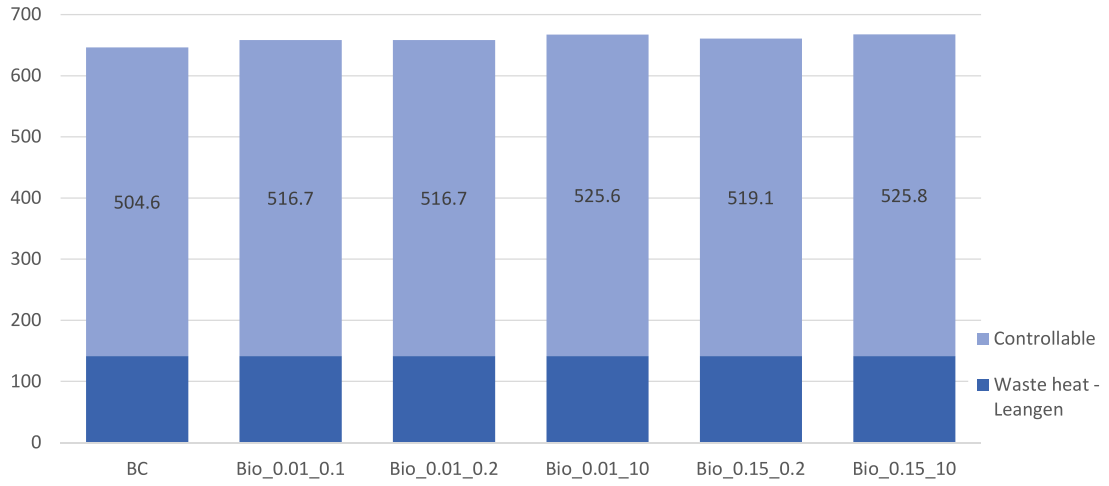

Fig. 3. Average heat generation by case (MWh).

Fuel costs account for about 80% of the total costs. The electricity costs for powering the heat pumps does not vary among the cases. Since electricity prices vary during the day, this was not an obvious outcome. Other operational characteristics drive the flexibility usage for HW supply, and variations in HW supply are not responsible for any differences between the cases. Inventory usage of seasonal TES is about 15% of total generation in all cases, and 10% higher in the cases not allowing curtailment compared to the cases allowing it. The amounts of shifted and curtailed hours are rather modest, with up to 2.7% and 1.1% respectively, but not negligible. The deficit costs in the no curtailment cases are much lower than in the cases that allow curtailment. Naturally, allowing curtailment means that higher deficits are possible too. For the cases that allow curtailment, the sum of deficit and curtailment cost is in the order of 1% of total costs.

Fig. 3 shows the total production for the six cases. In all cases, the ice rink supplies 141.7 MWh waste heat, about 27% of total generation. Compared to the Base Case, using storage increases production levels due to losses, while curtailing demand decreases generation levels. Total controllable generation is 2.4% to 4.2% higher.

Notably, cases Bio_0.01_0.1 & Bio_0.01_0.2 result in the exact same operational decisions, generation, and curtailment (but naturally twice as high curtailment costs for the latter case). Since the insights are the same, we ignore case Bio_0.01_0.1 in most of the following.

Fig. 4 shows the development over time of the average stored heat in the seasonal TES. The built-up of inventory is the same for all four cases until August. To avoid the implied cost from heat losses on the heat inventory, only surplus waste heat is stored. This changes in August. In August, the bio boiler can be used for additional storage. Additionally, the colder months are approaching, and losses on stored inventory do not chip away too much on potential cost savings. By the end of August, we observe two effects. First, in the cases that do not allow curtailment (and therefore use storage most), storage is filled to higher levels than in the cases that do allow curtailment. Second, the inventory levels for the cases with the low hourly deficit costs (0.01) are somewhat below the inventory levels for the cases with the high hourly deficit costs (0.15). Starting September, the average withdrawal patterns, reflected as the decrease in inventory levels in Fig. 4, are very similar, with the largest withdrawals in the coldest months. Since these values are

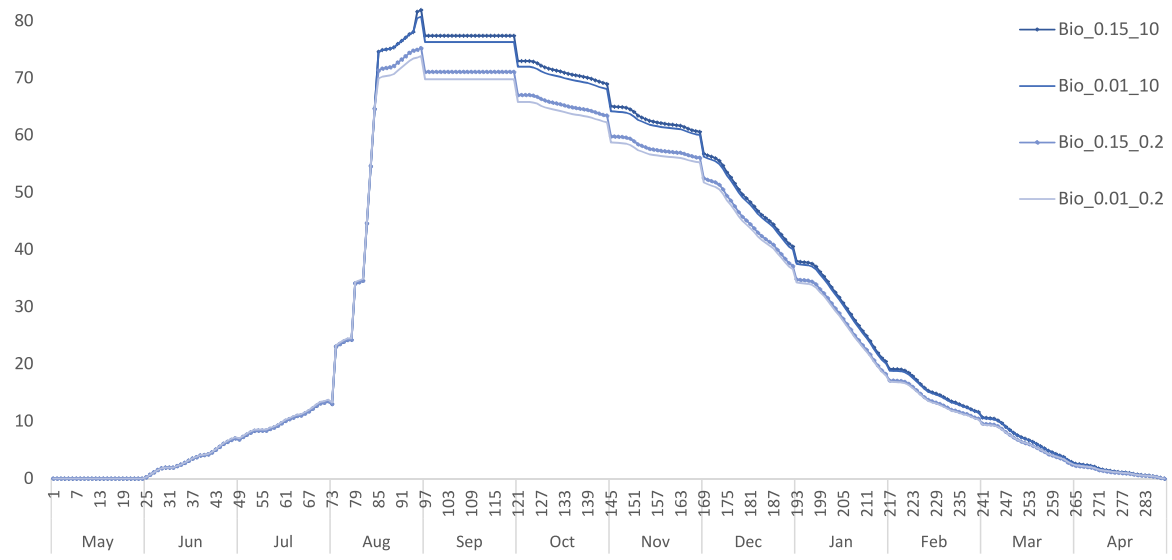

Fig. 4. Average inventory over time by case (MWh). Note that inventory drops at each transition to the next month due to heat loss (c.f., Constraints (8b)–(8a)).

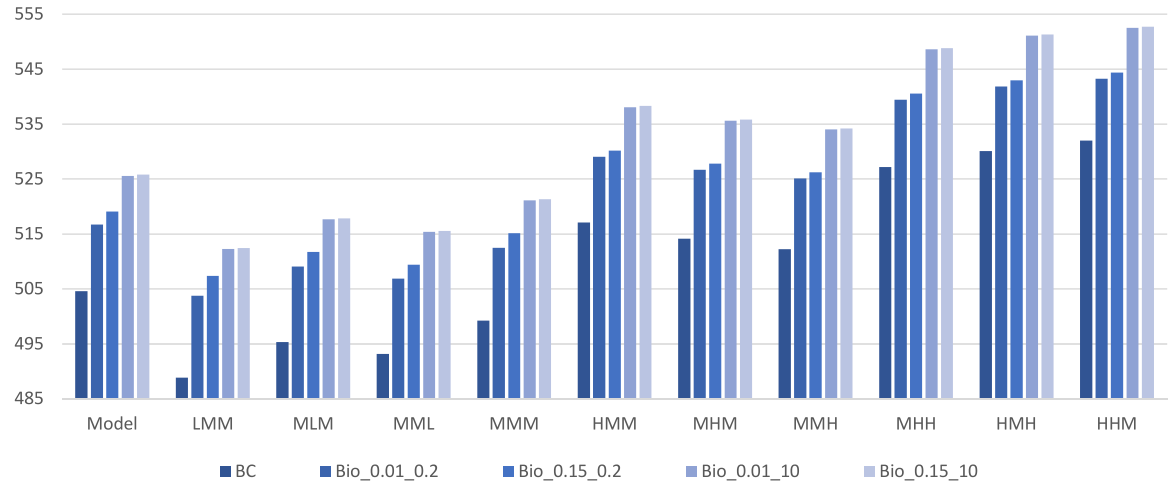

Fig. 5. Controllable generation for selected scenarios (MWh). Vertical axis truncated for comparability.

averages over all 6561 scenarios and give rather general insight only, we home in on detailed results next.

To illustrate the dynamics of the operations, we have lifted the specific results from ten of the 6561 scenarios. These scenarios consider combinations of low, medium, and high demand in the months January, February and March. Here, letter combinations indicate the variation using first letters. For instance, MMM means medium demand in all three months, while HLM means high demand in January, low demand in February, and medium demand in March.

Figs. 5 and 6 show production and CO_2 emission levels respectively for model average to the left, and all cases for the ten selected scenarios. Notably, in the medium scenario (MMM, the fifth group of columns) generation and CO_2 emissions are lower than the respective model average values. This is due to asymmetry in both uncertainty and in costs. Structurally, the generation in the no curtailment cases (the two right columns in each group) is highest, generation in the Base Case is always lowest, and the generation in two cases allowing curtailment are somewhat in the middle; the one with lowest deficit costs has somewhat lower generation than the other.

The CO_2 emission results have a different pattern. Here the cases not allowing curtailment have lower CO_2 emissions (in absolute terms) in the moderately low demand scenarios, but a little higher in the higher demand scenarios. This is due to the usage of storage. Storage is filled considering all the demand scenarios and their probabilities to occur. When a low demand scenario plays out, storage inventory is relatively high in later months, and can be used to replace more expensive, more polluting generation to meet demand. In contrast, in high demand scenarios, inventory is relatively low in later months, and therefore more costly and polluting peak generation is needed to meet demand.

To zoom further into details of the results, as an example Fig. 7 shows the supply mix for the same ten selected scenarios just for Case Bio_0.15_0.2. Consider April, which has the same demand in all depicted scenarios. Because of this, in April it is due to the different storage withdrawals in previous months that the supply mix in April is different in different scenarios. In the six scenarios where at least one of the three months of Jan, Feb or March had high demand, storage is empty after March, and all the supply in April comes from production.

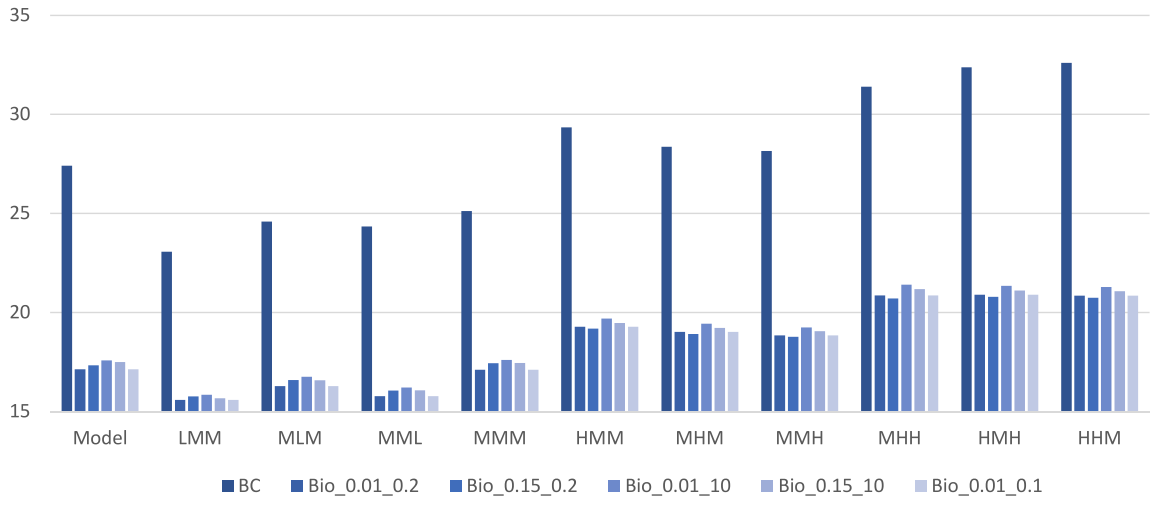

Fig. 6. CO_2 emissions (ton) for selected scenarios. Vertical axis are truncated for comparability.

In the other four scenarios (and in the model average) there is still some stored heat available to meet the demand in April. Interestingly, in the four scenarios where total supply in April from storage is highest, the total supply in April is also highest. This indicates that in the other six scenarios some curtailment occurs. We can conclude that this curtailment is cheap enough to prevent using peak generation technologies, but will be avoided if any stored heat is still available.

Next, Fig. 8 shows for Case Bio_0.15_0.2 the hourly and accumulative deficits for each representative day. The accumulative deficit by the last hour of the day, i.e., the end point of the line for each month, reflects the curtailment. Here we see the following pattern. Early in the day, deliveries are larger than demand and a supply surplus is built up. In the morning, between 6 am and 9 am, hourly supply becomes smaller than demand. Several (sometimes many) hours later, the accumulative surplus becomes an accumulative deficit. Later in the day, some time before the evening peak, deliveries become larger than demand again, and accumulative deficits become smaller. In the evening peak some deficits occur, and later in the evening some surpluses occur again. Over the entire day, in months May-Sep, surpluses and deficits balance each other out, and there is no curtailment. In all other months, over the day the deficits outweigh the surpluses, resulting in curtailment.

For completeness, we report the Values of the Stochastic Solution (VSS) for the reported cases. The VSS is a commonly used measure to evaluate the gain of using a stochastic model considering uncertainty (Recourse Solution, RS) compared to a deterministic model using the expected inputs, the expected value solution (EVS). In two-stage models this is done by fixing the first-stage variables in the stochastic model on the deterministic solution values, and run the model to evaluate the second stage optimal outcomes. This gives the so-called EEV.[2] The VSS is then the RS minus EEV. Since we have a multi-stage model with only storage inventory levels linking consecutive periods, we have opted to calculate the VSS by fixing inventory levels based on deterministic model outcomes at the end of August, just before the first uncertainty materializes in the stochastic problem. These values, and resulting VSS values are shown in Table 9.

Table 9 shows that the inventory by the end of summer in the stochastic model is always higher by about 10%–20%, but the overall cost differences, and therefore the VSS values, are very low. There are several reasons for this. The VSS tends to be low in problems with many stages, and many scenarios, if scenarios have long deterministic tails, and if the consequences of up and downward deviations are quite symmetrical. Additionally, fixing only one value in a large stochastic model allows it still a lot of freedom to optimize. Here, due to the high loss rates, the benefit of extra storage is most significant if a very cheap heat source can be used. Waste incineration is at capacity, so any additional heat storage comes from the somewhat, but not very, cheap Bio boiler. Therefore using stored heat is most beneficial, if it prevents the usage of the most expensive technology, LPG, and if that happens early winter, when losses have not compounded much yet. The number of hours that LPG is needed in early winter are limited. So the relative cost benefit of storage is modest. Still, considering the analyses presented above, we believe that a stochastic approach, especially when considering DSM as an additional flexibility option, is beneficial to optimize operations and determine optimal storage inventory levels.

Table 9
VSS with deterministic storage inventory at the end of August fixed in stochastic model.

Cases	Inventory [MWh]		EEV	SP	VSS	Δ
	Determ	Stoch				
Bio_0.01_10	72.4	80.7	159 295	159 221	74	0.05%
Bio_0.15_10	74.6	81.9	159 368	159 312	56	0.03%
Bio_0.01_0.2	65.0	73.9	157 839	157 753	86	0.05%
Bio_0.15_0.2	63.4	75.2	158 860	158 791	69	0.04%

6. Conclusion

This paper has presented a stochastic multi-stage optimization model for the tactical-operational planning of low-temperature District Heating Networks considering Demand Side Management and seasonal storage, and applied this to a case study for a new low-temperature district heating network under development in Trondheim, Norway. Through optimization and evaluation over an extensive number of scenarios generated based on uncertainty in space heating demand, we have compared the effect of varying deficit and curtailments costs on the generation mix, carbon dioxide emissions, operational costs and utilization of seasonal storage. Demand Side Management allows shifting some supply within a day, and some curtailment. This reduces the usage of peak generation technologies to some extent. Seasonal storage allows shifting supply from cold months to warmer months, which also reduces peak technology generation, and additionally a better utilization of very cheap technologies such as waste incineration with overcapacity in summer. For the case study, we found about 37% reduction in carbon dioxide emissions, 29% generation reduction in peak hours, and 10% lower operational costs due to storage and demand side management. Compared to a deterministic model, the

[2] The Expected value of the Expected-Value solution.

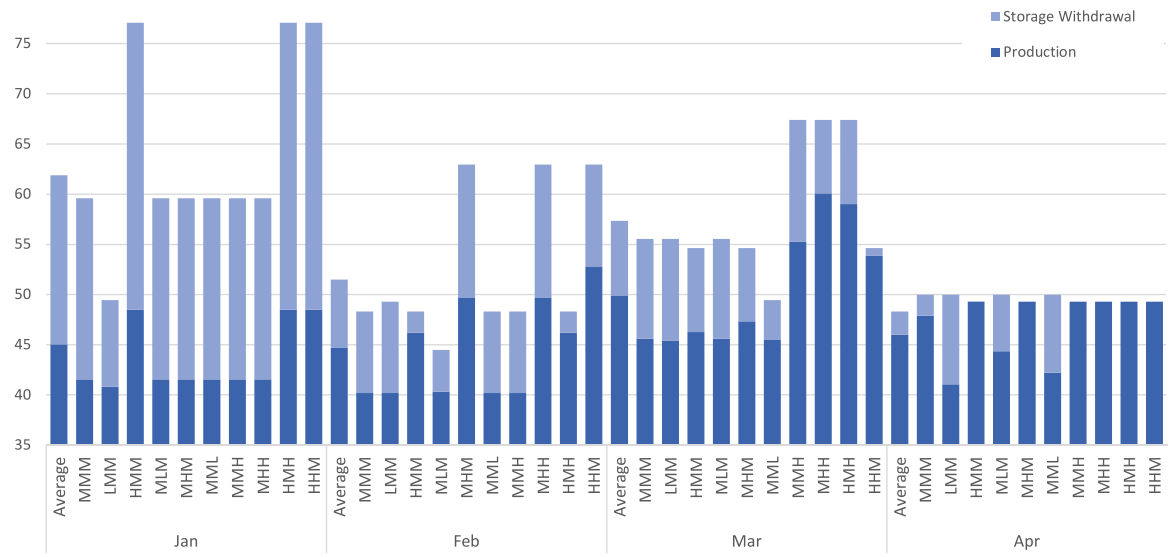

Fig. 7. Monthly supply mix for selected scenarios in Bio_0.15_0.2 (MWh). Vertical axis truncated for comparability.

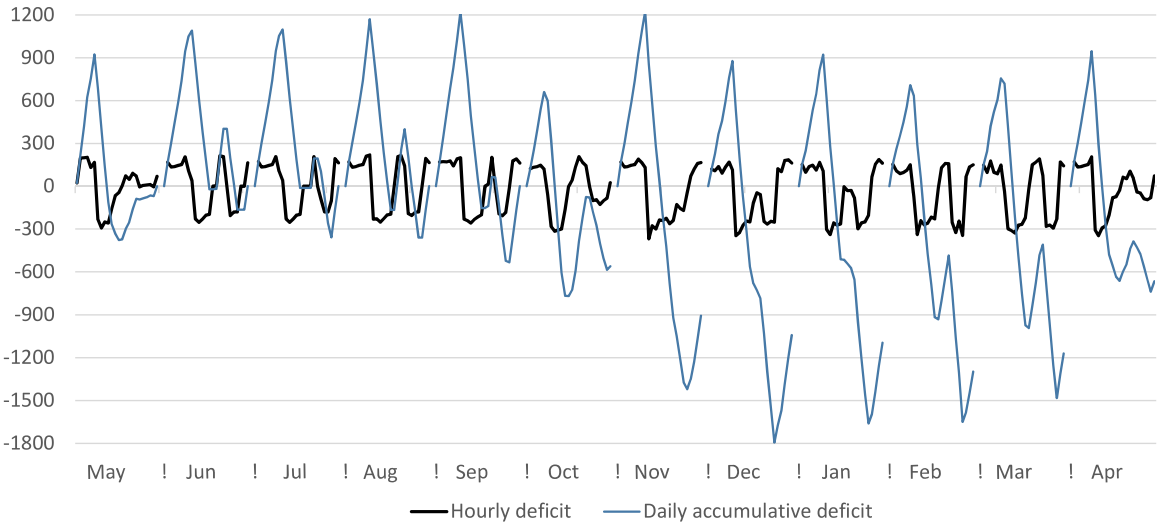

Fig. 8. Average hourly and accumulative deficits and surpluses (kWh) by representative day in case Bio_0.15_0.2.

stochastic model stores higher amounts of heat, but the overall differences in expected costs are low, mainly due the limited availability of very cheap heat sources in summer, the large number of stages, and the very large number of scenarios.

CRediT authorship contribution statement

Ruud Egging-Bratseth: Conceptualization, Formal analysis, Supervision, Visualization, Writing - original draft, Writing - review & editing. **Hanne Kauko:** Conceptualization, Supervision, Writing - original draft, Writing - review & editing. **Brage Rugstad Knudsen:** Conceptualization, Supervision, Writing - original draft, Writing - review & editing. **Sara Angell Bakke:** Conceptualization, Data curation, Investigation, Methodology, Software, Validation, Writing - original draft. **Amina Ettayebi:** Conceptualization, Data curation, Investigation, Methodology, Software, Validation, Writing - original draft. **Ina Renate Haufe:** Conceptualization, Data curation, Investigation, Methodology, Software, Validation, Writing - original draft.

Acknowledgments

The research leading to this publication has received funding from the project LTTG+ – Low-Temperature Thermal Grids with Surplus Heat Utilization (Grant number 280994). Hanne Kauko and Brage Rugstad Knudsen gratefully acknowledge the financial support from the Research Council of Norway and the user partners Statkraft Varme, Fortum Oslo Varme and Koteng Eiendom, as well as the municipalities of Gjøvik and Trondheim.

Ruud Egging-Bratseth acknowledges support from the Norwegian Research Council, grant 296205 Norwegian Centre for Energy Transition Strategies (FME NTRANS).

Appendix. Hourly temperature profiles

Demand for space heating depends very much on outdoor temperatures. The lower the temperatures are compared to the desired indoors temperature of about 21 °C, the higher the demand for space

Table 10
Hourly temperatures and scenario probabilities. Yearly scenarios are combinations of monthly scenarios.

Month	Jul	Aug	Sept			Oct			Nov			Dec		
Scen			Low	Med	High	Low	Med	High	Low	Med	High	Low	Med	High
Day average	13.83	13.67	8.55	9.30	14.07	1.85	4.90	8.56	−3.99	0.37	3.60	−6.81	−1.16	2.03
Probability	1.00	1.00	0.37	0.40	0.23	0.35	0.26	0.39	0.20	0.47	0.33	0.32	0.39	0.29
Hour 1	11.31	11.20	6.28	7.87	12.36	1.54	2.80	7.18	−5.03	0.49	2.51	−7.15	−1.95	2.93
Hour 2	10.49	10.50	5.77	7.48	11.64	1.16	2.06	6.89	−5.25	0.29	2.16	−7.39	−2.18	2.49
Hour 3	9.64	10.02	5.48	7.09	11.14	0.84	1.39	6.58	−5.58	−0.01	1.81	−7.62	−2.49	2.06
Hour 4	9.84	9.83	5.21	6.89	10.71	0.68	1.03	6.44	−5.72	−0.22	1.60	−7.85	−2.83	1.64
Hour 5	10.32	9.93	5.00	6.67	10.44	0.44	0.63	6.31	−5.93	−0.39	1.41	−7.96	−3.02	1.40
Hour 6	11.00	10.52	5.01	6.53	10.54	0.31	0.36	6.20	−6.15	−0.46	1.24	−8.12	−3.15	1.17
Hour 7	11.79	11.25	5.61	6.73	11.40	0.22	0.36	6.11	−6.25	−0.60	1.09	−8.27	−3.31	0.93
Hour 8	12.59	12.10	6.59	7.66	12.29	0.20	1.71	6.37	−6.37	−0.68	0.97	−8.35	−3.39	0.77
Hour 9	13.45	13.11	7.81	8.75	13.27	0.97	3.36	7.73	−6.00	−0.78	1.04	−8.38	−3.50	0.58
Hour 10	14.24	13.99	8.94	9.73	14.31	1.82	5.18	8.80	−4.37	−0.65	2.76	−8.48	−3.49	0.40
Hour 11	14.97	14.84	10.00	10.52	15.33	2.62	6.79	9.78	−3.13	0.53	4.50	−8.14	−1.29	0.78
Hour 12	15.66	15.59	10.94	11.22	16.00	3.20	7.94	10.77	−2.02	1.29	5.80	−5.78	0.05	2.80
Hour 13	16.20	16.18	11.46	11.85	16.41	3.58	8.76	11.24	−1.10	1.92	6.59	−4.61	0.55	3.67
Hour 14	16.58	16.65	11.99	12.19	17.19	3.95	9.53	11.51	−0.67	1.96	6.98	−4.21	0.60	3.61
Hour 15	16.80	16.94	12.24	12.24	17.53	3.93	9.83	11.37	−1.07	1.26	6.54	−5.57	0.63	2.74
Hour 16	16.89	17.05	12.17	12.09	17.61	3.56	9.55	10.93	−2.18	1.11	5.32	−5.68	0.35	2.68
Hour 17	16.84	16.97	11.81	11.63	17.43	2.92	8.71	10.25	−2.50	0.99	5.04	−5.81	0.56	2.59
Hour 18	16.65	16.65	11.14	10.97	17.04	2.65	7.40	9.78	−2.85	0.84	4.81	−5.92	0.83	2.49
Hour 19	16.19	16.12	10.29	10.32	16.26	2.38	6.74	9.41	−3.15	0.70	4.61	−6.04	0.56	2.42
Hour 20	15.61	15.45	9.67	9.88	15.44	2.09	6.08	9.03	−3.52	0.54	4.39	−6.18	0.29	2.31
Hour 21	15.00	14.68	9.00	9.43	14.61	1.77	5.35	8.71	−3.77	0.44	4.15	−6.32	0.00	2.24
Hour 22	14.30	13.84	8.26	8.97	13.77	1.55	4.73	8.40	−4.07	0.29	3.89	−6.44	−0.24	2.13
Hour 23	13.44	12.87	7.61	8.50	12.94	1.20	4.05	8.03	−4.37	0.14	3.69	−6.56	−0.55	2.02
Hour 24	12.19	11.89	6.95	8.01	12.07	0.92	3.36	7.70	−4.72	−0.01	3.41	−6.64	−0.78	1.90

Month	Jan			Feb			Mar			Apr			May	Jun
Scen	Low	Med	High	Low	Med	High	Low	Med	High	Low	Med	High		
Day average	−8.40	−2.14	1.47	−5.79	−0.56	0.80	−3.90	0.66	2.79	0.21	3.36	6.05	7.43	11.12
Probability	0.26	0.52	0.23	0.32	0.25	0.43	0.35	0.29	0.35	0.17	0.47	0.37	1.00	1.00
Hour 1	−7.40	−0.09	1.71	−5.73	−0.34	−0.78	−4.68	−0.82	0.23	−1.86	0.86	4.18	4.62	8.66
Hour 2	−7.86	−0.50	1.53	−6.22	−0.70	−1.18	−5.02	−1.24	−0.35	−2.32	0.20	3.62	3.83	7.71
Hour 3	−8.21	−0.81	1.36	−6.61	−1.06	−1.63	−5.26	−1.68	−0.80	−2.72	−0.17	3.30	3.05	6.78
Hour 4	−8.61	−1.13	1.17	−6.87	−1.33	−1.84	−5.45	−1.90	−1.03	−2.98	−0.44	3.02	3.14	7.11
Hour 5	−8.86	−1.26	1.07	−7.07	−1.59	−2.07	−5.66	−2.17	−1.29	−3.18	−0.39	2.79	3.61	7.60
Hour 6	−9.08	−1.41	0.99	−7.30	−1.67	−2.23	−5.73	−2.30	−1.41	−3.22	0.17	2.92	4.28	8.26
Hour 7	−9.31	−1.55	0.87	−7.46	−1.84	−2.36	−5.79	−2.24	−1.06	−2.66	0.92	3.66	5.13	9.05
Hour 8	−9.49	−1.66	0.81	−7.62	−1.99	−2.38	−5.65	−1.59	0.16	−1.84	1.86	4.60	6.05	9.90
Hour 9	−9.66	−1.74	0.76	−7.59	−2.06	−1.55	−4.81	−0.56	1.55	−0.88	3.00	5.53	7.00	10.67
Hour 10	−9.84	−1.42	0.70	−6.70	−1.53	0.06	−3.94	0.60	3.02	0.10	4.03	6.38	7.97	11.52
Hour 11	−9.03	−1.03	1.03	−5.72	−0.51	1.75	−3.15	1.66	4.35	1.10	4.94	7.19	8.84	12.30
Hour 12	−8.10	−1.19	2.33	−4.69	0.29	3.05	−2.60	2.58	5.48	2.12	5.72	7.91	9.51	12.89
Hour 13	−7.38	−1.35	2.86	−4.11	0.80	3.88	−2.11	3.26	6.37	2.76	6.31	8.41	10.10	13.43
Hour 14	−7.06	−2.51	3.01	−3.71	1.33	4.37	−1.73	3.73	6.95	3.22	6.60	8.86	10.52	13.85
Hour 15	−7.80	−2.67	2.31	−3.60	1.40	4.41	−1.65	3.93	7.21	3.54	6.83	9.15	10.76	14.11
Hour 16	−7.95	−2.83	2.14	−3.91	0.93	4.08	−1.77	3.82	7.15	3.64	6.86	9.23	10.83	14.20
Hour 17	−8.01	−2.99	1.97	−4.66	0.31	3.26	−2.22	3.34	6.66	3.40	6.64	9.03	10.76	14.11
Hour 18	−8.09	−3.14	1.80	−4.94	0.10	2.55	−2.81	2.64	5.85	2.92	6.14	8.58	10.41	13.85
Hour 19	−8.15	−3.30	1.61	−5.22	−0.10	2.18	−3.14	1.90	4.82	2.16	5.49	7.92	9.95	13.44
Hour 20	−8.26	−3.46	1.46	−5.34	−0.34	1.84	−3.49	1.44	4.09	1.34	4.71	7.18	9.29	12.86
Hour 21	−8.28	−3.62	1.27	−5.59	−0.57	1.48	−3.79	1.00	3.35	0.86	3.88	6.45	8.61	12.26
Hour 22	−8.33	−3.78	1.07	−5.96	−0.77	1.08	−4.09	0.58	2.61	0.36	3.03	5.80	7.78	11.62
Hour 23	−8.38	−3.94	0.91	−6.03	−1.01	0.78	−4.40	0.14	1.86	−0.12	2.14	5.09	6.65	10.98
Hour 24	−8.48	−4.10	0.60	−6.28	−1.26	0.45	−4.73	−0.30	1.10	−0.60	1.26	4.40	5.53	9.63

heating. Note that we assume space heating demand in months May–September as well as hot water demand in all months to not be subject to uncertainty.

References

[1] IEA. World energy outlook 2019. 2019.

[2] Connolly D, Mathiesen BV, Østergaard PA, Möller B, Nielsen S, Lund H, et al. Heat Roadmap Europe 2050: First pre-study for the EU27. 2012.

[3] ReUseHeat. The ReUseHeat project. 2020, [Accessed: 2020-06-24].

[4] Lund H, Werner S, Wiltshire R, Svendsen S, Thorsen JE, Hvelplund F, et al. 4th Generation District Heating (4GDH). Energy 2014;68:1–11.

[5] Guelpa E, Verda V. Thermal energy storage in district heating and cooling systems : A review. Appl Energy 2019;252:113474.

[6] Hennessy J, Li H, Wallin F, Thorin E. Flexibility in thermal grids: A review of short-term storage in district heating distribution networks. In: 10th international conference on applied energy, vol. 158. Hong Kong, China; 2019, p. 2430–4.

[7] Nordell B. Borehole heat store design optimization [Ph.D. thesis], Luleå tekniska universitet; 1994.

[8] Mesquita L, McClenahan D, Thornton J, Carriere J, Wong B. Drake landing solar community: 10 years of operation. In: ISES conference proceedings; 2017. p. 1–2.

[9] Nordell B, Andersson O, Rydell L, Scorpo AL. Long-term performance of the HT-BTES in Emmaboda, Sweden. In: Greenstock 2015: International conference on underground thermal energy storage 19/05/2015-21/05/2015; 2015.

[10] Vandermeulen A, van der Heijde B, Helsen L. Controlling district heating and cooling networks to unlock flexibility: A review. Energy 2018;151:103–15.

[11] Leśko M, Bujalski W, Futyma K. Operational optimization in district heating systems with the use of thermal energy storage. Energy 2018;165:902–15.

[12] Verrilli F, Srinivasan S, Gambino G, Canelli M, Himanka M, Del Vecchio C, et al. Model predictive control-based optimal operations of district heating system with thermal energy storage and flexible loads. IEEE Trans Autom Sci Eng 2017;14(2):547–57.

[13] Knudsen MD, Petersen S. Model predictive control for demand response of domestic hot water preparation in ultra-low temperature district heating systems. Energy Build 2017;146:55–64.
[14] Vivian J, Quaggiotto D, Zarrella A. Increasing the energy flexibility of existing district heating networks through flow rate variations. Appl Energy 2020;275(February):115411.
[15] Zheng J, Zhou Z, Zhao J, Wang J. Integrated heat and power dispatch truly utilizing thermal inertia of district heating network for wind power integration. Appl Energy 2018;211(November 2017):865–74.
[16] Claessens BJ, Vanhoudt D, Desmedt J, Ruelens F. Model-free control of thermostatically controlled loads connected to a district heating network. Energy Build 2018;159:1–10.
[17] Van Der Meulen S. Load management in district heating systems. Energy Build 1988;12:179–89.
[18] Wernstedt F, Davidsson P, Johansson C. Demand side management in district heating systems. In: Proceedings of the international conference on autonomous agents, vol. 5. 2007, p. 1383–9.
[19] Guelpa E, Marincioni L, Deputato S, Capone M, Amelio S, Pochettino E, et al. Demand side management in district heating networks: A real application. Energy 2019;182:433–42.
[20] Cai H, Ziras C, You S, Li R, Honoré K, Bindner HW. Demand side management in urban district heating networks. Appl Energy 2018;230:506–18.
[21] Sweetnam T, Spataru C, Barrett M, Carter E. Domestic demand-side response on district heating networks. Buil Res Inf 2019;47(4):330–43.
[22] Ala-Kotila P, Vainio T, Heinonen J. Demand response in district heating market—Results of the field tests in student apartment buildings. Smart Cities 2020;3(2):157–71.
[23] Vand B, Martin K, Jokisalo J, Kosonen R, Hast A. Demand response potential of district heating and ventilation in an educational office building. Sci Technol Built Environ 2020;26(3):304–19.
[24] Hohmann M, Warrington J, Lygeros J. A two-stage polynomial approach to stochastic optimization of district heating networks. Sustain Energy Grids Netw 2019;17:100177.
[25] Blanco I, Guericke D, Morales JM, Madsen H. A two-phase stochastic programming approach to biomass supply planning for combined heat and power plants. OR Spectrum 2020.
[26] Zhang M, Wu Q, Wen J, Pan B, Qi S. Two-stage stochastic optimal operation of integrated electricity and heat system considering reserve of flexible devices and spatial-temporal correlation of wind power. Appl Energy 2020;275(April):115357.
[27] Dorotić H, Pukšec T, Duić N. Multi-objective optimization of district heating and cooling systems for a one-year time horizon. Energy 2019;169:319–28.
[28] Sameti M, Haghighat F. Optimization of 4th generation distributed district heating system: Design and planning of combined heat and power. Renew Energy 2019;130:371–87.
[29] Vesterlund M, Toffolo A, Dahl J. Optimization of multi-source complex district heating network, a case study. Energy 2017;126:53–63.
[30] Brand M, Svendsen S. Renewable-based low-temperature district heating for existing buildings in various stages of refurbishment. Energy 2013;62:311–9.
[31] Sidelnikova M, Weir DE, Groth LH, Nybakke K, Stensby KE, Langseth B, et al. Kostnader i energisektoren - Kraft, varme og effektivisering. 2015.
[32] Kauko H, Kvalsvik KH, Rohde D, Hafner A, Nord N. Dynamic modelling of local low-temperature heating grids: A case study for Norway. 2017.
[33] NordPool. Historical market data- elspot prices -hourly. 2020, [Accessed 2020-02-14].
[34] Tvärne A. Värmeförsörjning i Furuset med utnyttjande av säsongslager i systemet. 2018, [unpublished].
[35] ProgramByggerne ANS. SIMIEN Wiki. 2020.